Three-Dimensional Cataract Crystalline Lens Imaging With Swept-Source Optical Coherence Tomography

Alberto de Castro,[1] Antonio Benito,[1] Silvestre Manzanera,[1] Juan Mompeán,[1] Belén Cañizares,[2] David Martínez,[2] Jose María Marín,[2] Ireneusz Grulkowski,[3] and Pablo Artal[1]

[1]Laboratorio de Óptica, Universidad de Murcia. Campus de Espinardo, Murcia, Spain
[2]Servicio de Oftalmología, Hospital Virgen de la Arrixaca, Ctra. Madrid-Cartagena, El Palmar, Murcia, Spain
[3]Institute of Physics, Faculty of Physics, Astronomy and Informatics, Nicolaus Copernicus University, Toruń, Poland

Correspondence: Pablo Artal, Laboratorio de Óptica, Universidad de Murcia, Campus de Espinardo, Edificio 34, 30100 Murcia, Spain; pablo@um.es.

Submitted: December 9, 2017
Accepted: January 15, 2018

Citation: de Castro A, Benito A, Manzanera S, et al. Three-dimensional cataract crystalline lens imaging with swept-source optical coherence tomography. *Invest Ophthalmol Vis Sci*. 2018;59:897–903. https://doi.org/10.1167/iovs.17-23596

Purpose. To image, describe, and characterize different features visible in the crystalline lens of older adults with and without cataract when imaged three-dimensionally with a swept-source optical coherence tomography (SS-OCT) system.

Methods. We used a new SS-OCT laboratory prototype designed to enhance the visualization of the crystalline lens and imaged the entire anterior segment of both eyes in two groups of participants: patients scheduled to undergo cataract surgery, $n = 17$, age range 36 to 91 years old, and volunteers without visual complains, $n = 14$, age range 20 to 81 years old. Pre–cataract surgery patients were also clinically graded according to the Lens Opacification Classification System III. The three-dimensional location and shape of the visible opacities were compared with the clinical grading.

Results. Hypo- and hyperreflective features were visible in the lens of all pre–cataract surgery patients and in some of the older adults in the volunteer group. When the clinical examination revealed cortical or subcapsular cataracts, hyperreflective features were visible either in the cortex parallel to the surfaces of the lens or in the posterior pole. Other type of opacities that appeared as hyporeflective localized features were identified in the cortex of the lens. The OCT signal in the nucleus of the crystalline lens correlated with the nuclear cataract clinical grade.

Conclusions. A dedicated OCT is a useful tool to study in vivo the subtle opacities in the cataractous crystalline lens, revealing its position and size three-dimensionally. The use of these images allows obtaining more detailed information on the age-related changes leading to cataract.

Keywords: cataract type, cataract models, optical coherence tomography, lens opacity

Cataract is the leading cause of blindness worldwide,[1] and is a condition characterized by the progressive loss of the transparency of the crystalline lens that results in visual impairment. Multiple factors, such as aging, disease, genetics, nutritional or metabolic deficiencies, trauma, congenital factors, and environmental stress (e.g., radiation), can contribute to the development of cataracts, with age being the major contributor.[2,3] Cataracts are classified according to their location or cause. Nuclear cataracts are characterized by an increase of light scattering in the nucleus of the crystalline lens and can be accompanied by a myopic shift and an increase in yellow coloration due to the absorption of wavelengths in the blue end of the spectrum. A cataract is called cortical when located in the cortex. These have typically a spike-like shape, are thicker in the periphery, progress slowly, and have been observed to expand to adjacent fiber cells.[2,4,5] A posterior subcapsular cataract is located just beneath the posterior capsule and affects vision significantly very early due to its location along the visual axis and close to the nodal point of the eye.[6]

In clinical practice, a slit lamp is routinely used to visualize the opaque lens and determine if the patient should undergo cataract surgery. Although this is ultimately decided by estimating the impact of the cataract in a patient's vision, different metrics have been proposed to quantify the opacities using slit lamp images with the purpose of evaluating its influence and studying its progression. The presence and severity of the cataract can be determined by trained graders comparing the photographs with a series of standards. Several of these systems exist,[1,7–10] and most of them are based on input data from slit lamp images. Although some are very complete but difficult to apply clinically,[7] others focus on the possibility to quickly evaluate the cataract in a simple and reproducible way[1,8] or are designed to grade a specific type of cataract.[10] Currently, the most widely used system is the Lens Opacities Classification System III (LOCS III),[9] which evaluates the cataract using slit lamp images of the lens with either direct focal or retro illumination. Direct focal illumination allows observing an image of a section of the lens. It is achieved by directing a bright thin beam of light obliquely into the eye and focusing it so that only a section of the lens is illuminated. Retro-illumination technique is used to obtain an aerial view of the opacities of cornea and lens and is performed by aligning the beam of light with the observation axis so that the light bounces off the fundus and returns to the observer back through the pupil. The cataracts are graded by comparing the observed images with a standard using four aspects: the nucleus opalescence (NO) and the nucleus color (NC), the

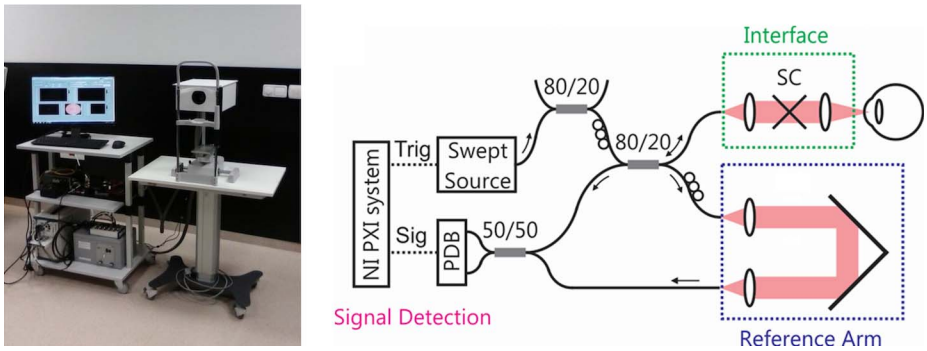

FIGURE 1. Photograph and scheme of the long-range SS-OCT setup at 1050 nm. A Thorlabs (Newton, NJ, USA) balanced photodetector (PDB) and a National Instruments (Austin, TX, USA) acquisition system (PXI) were used to detect and acquire the interferometric signal. Galvanometric scanners (SC) enabled lateral beam scanning of the eye.

cortical cataract (C), and the posterior subcapsular cataract (P). Although the first two values, NO and NC, evaluate the scattering properties of the nucleus, C and P are estimations of the percentage of the pupillary area occupied by the cortical or subcapsular opacities, respectively.

Other imaging techniques, such as Scheimpflug imaging or optical coherence tomography (OCT), also have been used extensively to obtain information of the crystalline lens. Different parameters to grade a given cataract using Scheimpflug have been proposed. For example, the number of images affected by cortical cataract[11] or the number of opaque pixels in the cortex[12] were suggested to evaluate the degree of cortical cataract, and although some studies showed that the average signal in the lens nucleus was shown to be related to the nuclear cataract grading,[12–15] other authors suggested that more complex metrics using the full shape of the image intensity profile with depth[16] should be used to correctly classify the opacity. OCT studies on cataract classification are not so common, but this imaging technique is becoming increasingly popular to study the anterior segment. Recently, some authors have proposed the use of cross-sectional two-dimensional OCT images to grade the scattering produced by the nucleus and have found a positive correlation with the LOCS III grading.[17,18] Also, in vivo OCT images of cataract crystalline lenses in Rhesus monkeys showed a direct correlation with the cataractous lesions seen on corresponding histopathologic sections, showing the potential of the imaging technique to identify and characterize cataracts.[19]

Although different metrics can be used to describe the cataract and determine its influence on vision, three-dimensional (3-D) volumetric imaging of the cataracts of the lens allows a comprehensive and detailed description of its shape, location, and size. Also, with enough resolution, the images would allow the study of small changes as the cataract evolves with time. In this article, we demonstrate, as far as we know for the first time, the use of 3-D imaging of the crystalline lens on volunteers without cataracts and on a set of patients with confirmed cataracts using swept-source OCT (SS-OCT) to study the shape, size, and location of the opacities that form in the crystalline lens of the aging human eye.

METHODS

Instrument: SS-OCT Imaging System

A custom long-range SS-OCT imaging system operating at the speed of 50 k A-scans/s was specifically designed to perform volumetric imaging of the entire anterior segment of the eye. Essentially, the light from a swept-source laser (Axsun Technologies, Billerica, MA, USA) with a central wavelength of 1050 nm and a sweep range of 100 nm was focused on the anterior segment of the eye, and the interference between the light backscattered from the eye and that from a reference beam was recorded using a balanced photodetector (Fig. 1). To 3-D image the anterior segment, two galvanometric scanners were used to move the beam following a raster pattern with a range set to either 8×8 mm^2 or 16×16 mm^2. The light incident in the eye was 1.9 mW, below the maximum permissible exposure established in the American National Standard for Safe Use of Lasers (ANSI Z136.1-2007). In each examination, several 3-D images were obtained with scan protocols that kept the imaging time below 1.9 seconds. A raster scan pattern with 1990×50 A-scans allowed high lateral-resolution images (4 μm and 8 μm for 8×8 mm^2 and 16×16 mm^2 imaging range, respectively), whereas a pattern with 300×300 A-scans allowed equal scan density in the horizontal and vertical axis (26 μm and 53 μm for 8×8 and 16×16 mm^2, respectively). The axial resolution of the OCT was 8 μm, and an imaging range of 22.2 mm in air was spanned over 4096 pixels in the OCT image.

Subjects

The anterior segment was studied in two groups of participants: 15 healthy volunteers without complaints about their vision (age range 13–81, mean 45 years old) and 16 pre-cataract surgery patients (age range 36–91, mean 67 years old) who had been selected by their ophthalmologist to undergo cataract surgery in a local hospital. All patients were imaged 2 weeks before surgery, and one to two drops of 1% Tropicamide was administered to dilate the pupil and paralyze accommodation.

After dilation, a clinical examination of the anterior segment was performed in the pre–cataract surgery patients with a slit lamp, and the opacity present in the crystalline lens was graded according to the LOCS III standard by an experienced ophthalmologist. Then, several 3-D volumetric images of the entire anterior segment were acquired with the SS-OCT. The complete examination time took less than 30 minutes. All practices and research adhered to the tenets of the Declaration of Helsinki and were approved by the institutional review boards of the University of Murcia. An informed consent was obtained from all the subjects in the study after explanation of the procedures and the possible consequences.

Image Analysis

A MATLAB (MathWorks, Natick, MA, USA) routine was written to load all the B scans corresponding to a 3-D volumetric data

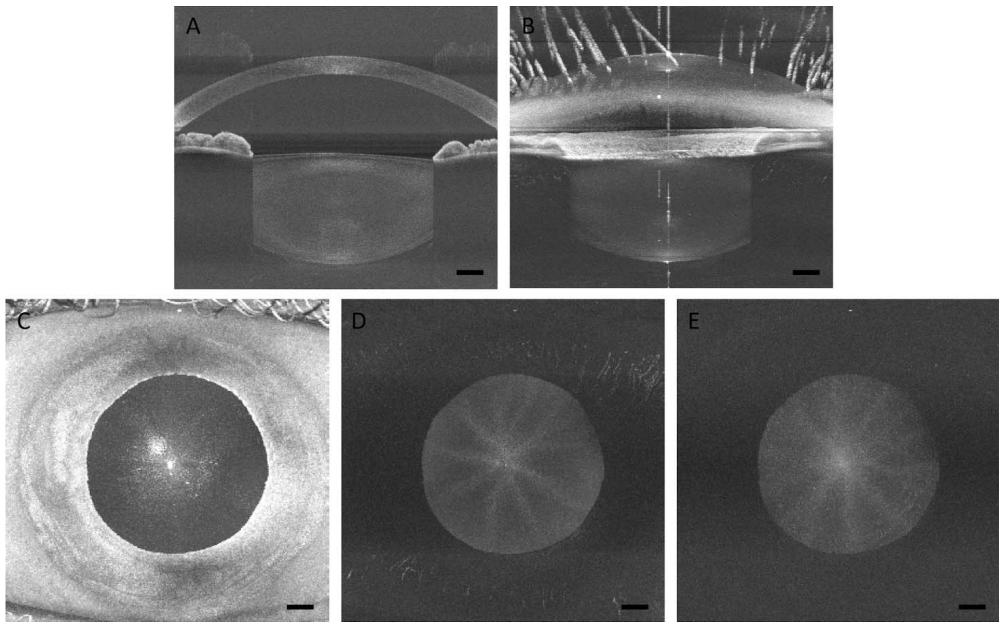

FIGURE 2. SS-OCT images of the anterior segment of a healthy 26-year-old male participant: central cross-section of the 3-D image (**A**), projection of the maximum intensity in the lateral direction (**B**) and in the axial direction (**C**), and axial projection of the maximum intensity of the anterior (**D**) and posterior (**E**) halves of the crystalline lens. Note that the reflex in the cornea and the lens are visible in (**C**) and that by selecting only the anterior part or posterior part of the lens, these can be avoided to visualize the sutures of the lens. *Scale bars*: 1 mm.

set, display them with the right aspect ratio, and project laterally or axially the maximum intensity. Either the whole volume or a section could be used to generate projection images (Fig. 2). The 1900 × 50 OCT images allowed the visualization of different horizontal sections of the lens in detail and the 300 × 300 images were used to construct the volumetric image and to project the maximum intensity either laterally or axially. From these series of images, 3D video clips of the anterior segment can be produced (see Supplementary Movie S1).

We observed hyper- and hyporeflective features in the lens of all the pre-cataract patients imaged. These seemed to correspond with different types of cataracts and were grouped visually by their similarity and their characteristics compared with the score in the LOCS III grading.

Additionally, a semiautomatic algorithm was developed to calculate the average OCT signal in the central area of the lens. Although the power of the SS laser and the working distance was kept constant, to account for possible differences in the signal strength, the average signal in the area behind the iris was used as a background. The pupil was manually segmented and the average signal in the A-scans corresponding to the central 1 mm was evaluated. The anterior and posterior lens surfaces appeared in the image densitometry curves as narrow spikes and were used to locate the crystalline lens. The percentage corresponding to the anterior cortex, nucleus, and posterior cortex was calculated using an age-dependent model[20] and the intensity of the OCT signal was compared with the LOCS III standard score. Pearson correlation coefficient was used to assess statistical significance.

RESULTS

Cataract Imaging

We observed hypo- and hyperreflective features in the crystalline lenses of every pre–cataract surgery patient. Because these were never observed in the images of young crystalline lenses, and due to their shape and because some of them blocked the OCT signal, we assumed that these structures corresponded to cataract opacities. Access to volumetric images enabled generation of the projections of the maximum intensity in the lateral and axial directions. Those projections allowed a better visualization of the opacities present in some of the lenses and a better understanding of the similarities and differences between them.

The most common and notable opacity extended parallel to either the anterior or the posterior surface of the lens and seemed to be more pronounced in the periphery of the pupil. These were always hyperreflective and probably corresponded to cortical cataracts. As an example, in Figure 3, the central B-scan and the 3-D projections in both the meridional and axial directions of an eye with a cortical cataract can be observed. We observed cortical cataracts in 13 of the 17 pre–cataract surgery patients studied, bilaterally on 6 of them. They were located in the anterior or the posterior cortex only in 3 and 5 lenses, respectively, and in both the anterior and the posterior cortex in 11 lenses. In one of the older participants without visual complaints (age 62), we identified one of these cataracts in the posterior cortex of the lens. In every pre–cataract surgery patient where these structures were observed, the cortical cataract grading of LOCS III was different from 1.

Subcapsular cataracts appeared in the OCT images as hyperreflective that grew next to the posterior capsule of the crystalline lens (Fig. 4). These were observed in 4 of 17 pre–cataract surgery patients, bilaterally in 1 of them. Small features that looked like small subcapsular cataracts were observed in two of the participans without visual complains, binocularly in one of them (age 62) monocularly in the other (age 81).

A different kind of feature that was observed only in pre–cataract surgery patients was hyporeflective localized areas that looked like defects in the crystalline lens tissue (Fig. 5).

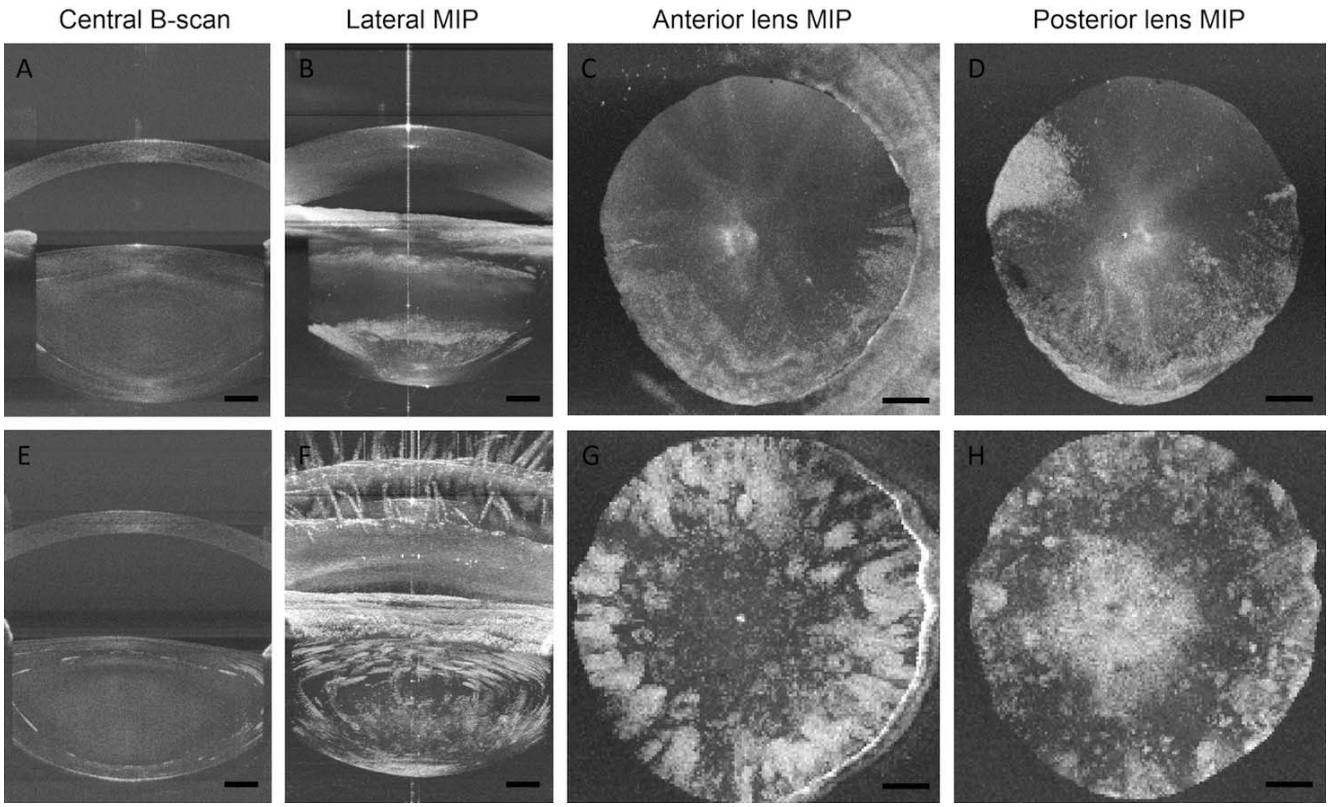

FIGURE 3. Cortical cataract imaged in the right eye of a 63-year-old (*top row*) and a 53-year-old (*bottom row*) female pre–cataract surgery patient. Central cross-section (**A**, **E**), lateral projection of the volume maximum intensity (**B**, **F**), and axial projection of the anterior (**C**, **G**) and the posterior (**D**, **H**) part of the crystalline lens. A 3-D view of the volumetric image of the 53-year-old patient can be seen in Supplementary Movie S1. The lateral projection of the maximum intensity allowed observing the extent of the opacities and their location either in the anterior or posterior cortex of the crystalline lens. *Scale bars*: 1 mm.

Their size, measured in the cross-sectional images, was relatively small (range, 20–200 μm). They were always located in the cortex of the crystalline lens and centered in the pupil.

Densitometry Measurements

The anterior and posterior cortex and the nucleus were identified in all the images, and the average OCT signal at the nucleus in the central 1 mm, which can be considered a measurement of the amount of light reflected and backscattered by the tissue in the area, was studied as a function of age and the nuclear opalescence grading on the LOCS III scale. We observed a statistically significant correlation between the average OCT signal in the nucleus of the lens and the nuclear opalescence grading on the LOCS III scale (Fig. 6A). Also, the values of OCT signal in the nucleus increase, on average, with age, indicating an increment on the scattering of the nucleus with age (Fig. 6B).

Discussion

We have performed volumetric imaging of the crystalline lens of pre–cataract surgery patients using a dedicated noncontact long-depth-range SS-OCT system. In the images, we were able to visualize different types of opacities and obtain precise information about their size and location in the crystalline lens. We used high-resolution B-scan images to observe two-dimensional sections of the lens and we projected the maximum intensity laterally and axially to improve the visualization of the opacities and to locate them in the lens.

Other imaging systems, such as Scheimpflug, have been used in the past to study the presence of cataracts in the crystalline lens. Problems related to the dynamic range of the sensor in different systems can be solved by calibrating the instrument with different neutral density filters to calculate the optical intensity instead of relying on the pixel intensity.[21] It was observed that different features of the lens correlated well with LOCS III grading and hence could be used to grade the cataract.[11–16] However, due to its configuration, blockage of eyelids and eyelashes can affect the intensity of Scheimpflug images, and the visible wavelength used can be absorbed by the cataract itself, decreasing densitometry values and the amount of light transmitted to deeper structures.[22] Using polarized light in biomicroscopy, it was shown that polarized light can be used to observe structures not visible with standard biomicroscopic techniques.[23] This suggests that polarization could improve the contrast when imaging cataracts with both Scheimpflug and OCT systems.

We have illustrated the appearance of different opacities in the crystalline lens of pre–cataract surgery patients in a comprehensive way when imaged with a 3-D volumetric SS-OCT. We computed the average OCT signal in the central 1 mm of the pupil and observed that the image intensity in the nucleus of the crystalline lens correlated well with the

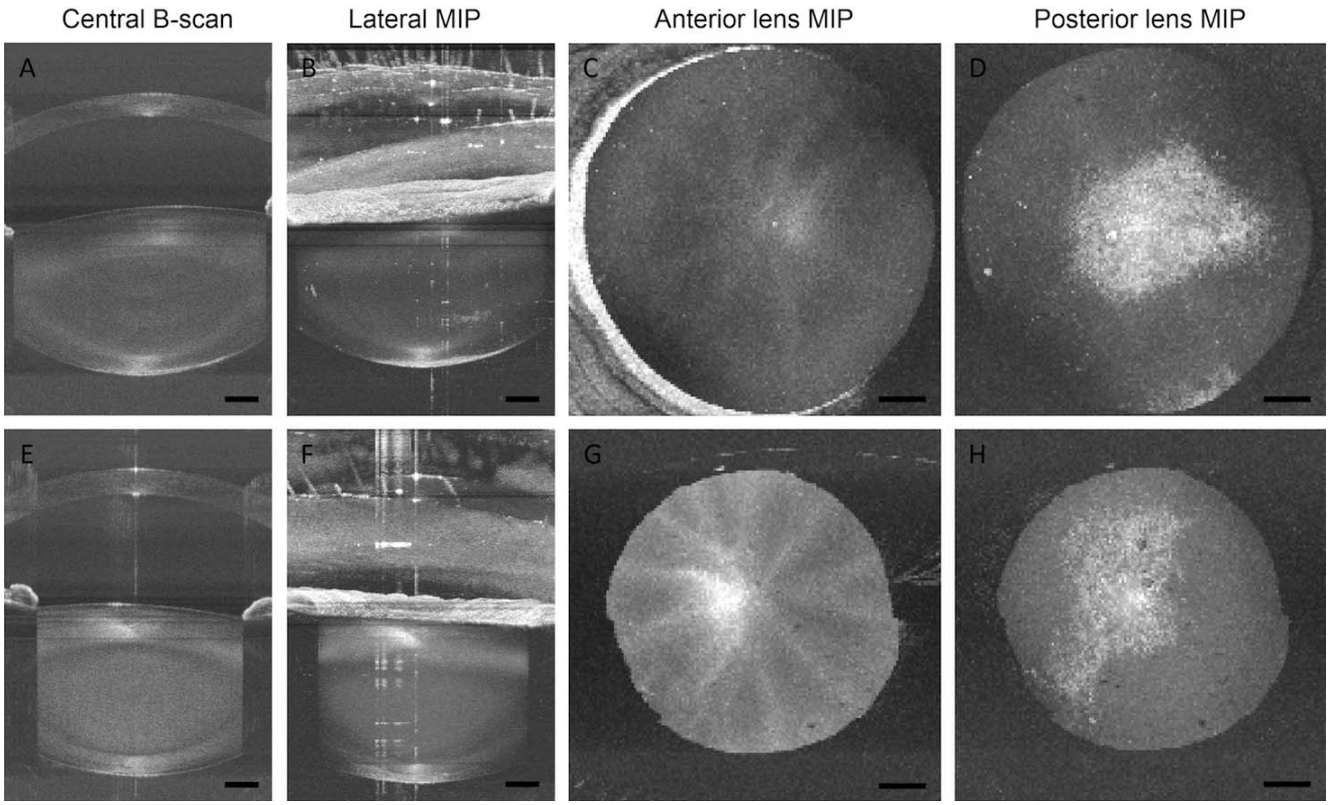

FIGURE 4. Posterior subcapsular cataract imaged with the SS-OCT in a 53-year-old (*top row*) and a 77-year-old (*bottom row*) pre–cataract surgery male patient. Central cross-section (**A**, **E**), lateral projection (**B**, **F**) of the maximum intensity, axial projection of the anterior (**C**, **G**), and the posterior (**D**, **H**) part of the crystalline lens. Although the anterior segment of the crystalline lens (**C**, **G**) seems normal, the observation of the posterior segment (**D**, **H**) reveals the shape and extent of the posterior subcapsular cataract. *Scale bars*: 1 mm.

subjective nuclear opalescence score assigned by an ophthalmologist using a slit lamp, suggesting that the average OCT signal in the nucleus can be informative of the degree of nuclear cataract in the crystalline lens. This was recently reported in studies in which the nucleus was semiautomatically detected in two-dimensional images of the anterior segment.[17,18] The SS-OCT system can rapidly acquire 3-D images of the crystalline lens using longer wavelengths, which should improve the images of the lens behind a cataract due to its better penetration. The intensity of the OCT signal can be used to quantify the scattering properties of the nucleus or other type of opacities, and the ability to rapidly obtain high-resolution 3-D images of the crystalline lens can help locating the cataract in both the axial and meridional plane, determining its size, the pupil area occupied by the opacity, or measuring small changes as the cataract develops. Finally, the images may be informative of the cataract hardness, as has been proved with other imaging techniques, such as ultrasound biometry or Scheimpflug camera. Using an ultrasound probe, acoustical parameters such as velocity, attenuation or backscattered signal were observed to be predictive of cataract hardness in animal models,[24–26] and the image intensity in the lens nucleus in Scheimpflug images was found to correlate with phacoemulsification time or average phacoemulsification power,[14,27] suggesting that imaging before the surgery may be useful to plan some of these parameters.

It can be argued that the OCT light wavelength is far from the visible wavelength and that the images are obtained due to the backscattering properties of the opacities and not the forward scattering, which is what the patient will finally experience. There are methods to calculate the amount of forward scattering in visible wavelengths either requiring participation from the subject using psychophysical techniques[28] or objectively with double pass images.[29] These methods can be used to determine the amount of forward scattering introduced by the ocular media and have been found to correlate well with the LOCS III classification system.[30] These indices do not determine where the scattering originates, but they calculate the magnitude of the intraocular scattering that can be used to estimate the influence in the image projected in the retina.

This study focused on imaging the cataracts and provided qualitative data on the location of the lens opacifications imaged with OCT systems, which is rapidly becoming a common technique to image the anterior segment. Although the advantage of SS-OCT modality includes access to volumetric information with micrometer resolution, the limitations of the study stem from the corneal specular reflection (which saturates the OCT images), as well as from the inability to visualize the crystalline lens behind the iris (the periphery of the lens is usually the place of formation of opacifications at early stages).

To summarize, 3-D SS-OCT enables comprehensive visualization of the opacifications of the crystalline lens in vivo, revealing their positions and sizes. The access to micrometer-resolution information on optical properties of the aging lens may allow a detailed study of the age-related changes leading to cataract.

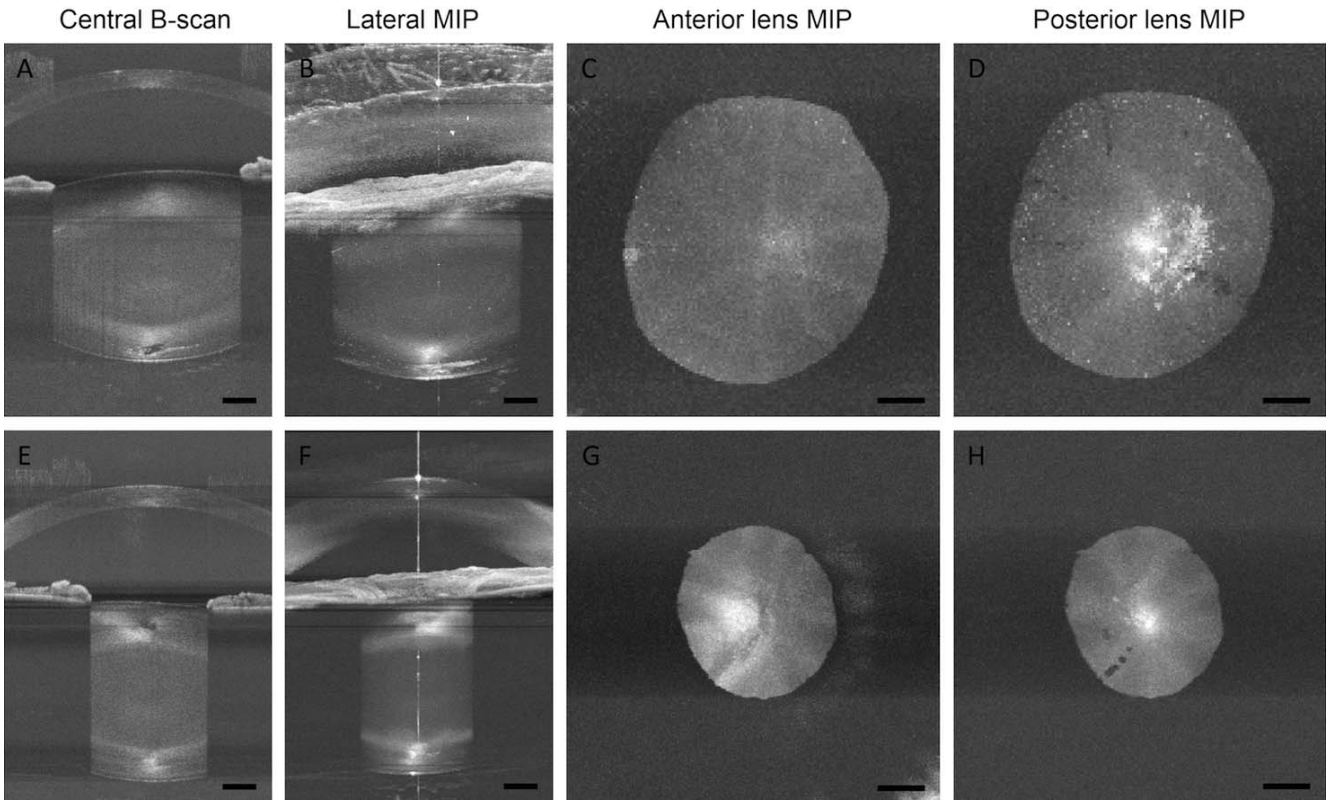

FIGURE 5. Hyporeflective localized structures localized in the posterior capsule of a 91-year-old female (**A–D**) and in the anterior capsule of a 69-year-old male (**E–H**). The hyporeflective defect can be clearly observed in the two-dimensional images (**A**, **E**), and the axial projection reveals the extent that, as can be seen in the second example (**G**), can be quite large. Shadows of the cataract can be observed in the projection of the posterior part of the lens (**H**). *Scale bars*: 1 mm.

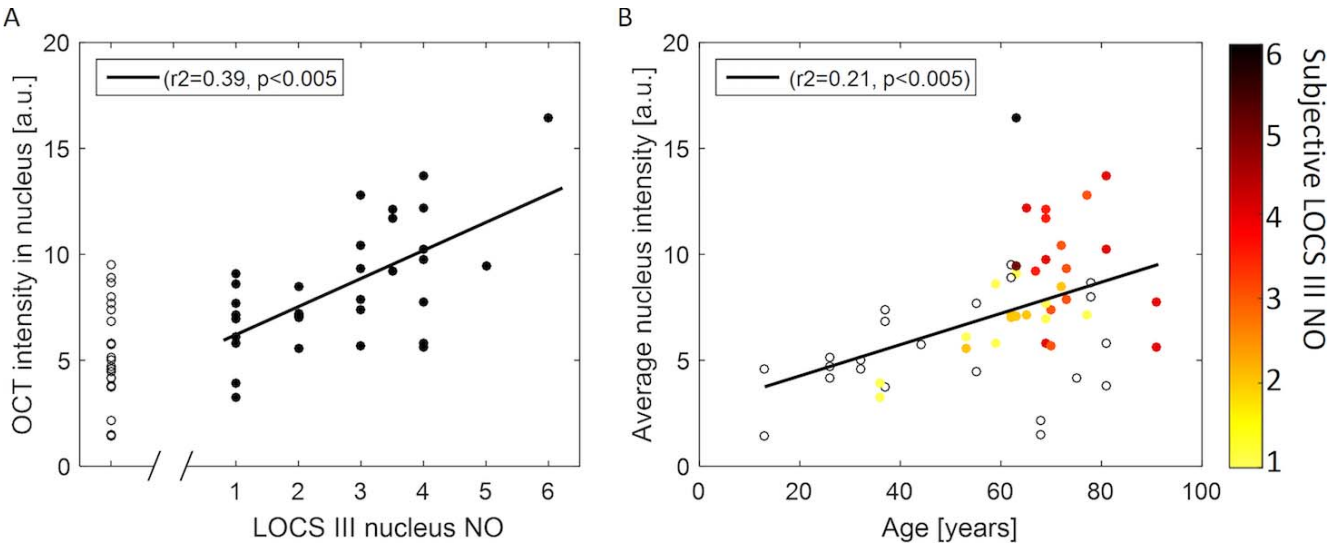

FIGURE 6. (**A**) Correlation between the OCT intensity in the nucleus and the clinical LOCS III grading. The intensity of the OCT signal in the non pre-cataract surgery patient crystalline lens images was added to the plot using empty symbols for comparison. (**B**) OCT signal in the nucleus as a function of age. The points were colored using the subjective NO LOCS III grade and empty symbols were used to represent participants without visual complains.

Investigative Ophthalmology & Visual Science

Acknowledgments

Supported by European Research Council Advanced Grant (ERC-2013-AdG-339228, SEECAT), Secretaría de Estado de Investigación, Desarollo e Innovación, Spain (SEIDI FIS2013-41237-R), Polish Ministry of Science and Higher Education (IUVENTUS PLUS, IP2014-014073), Fundación Séneca, Murcia, Spain (19897/GERM/15).

Disclosure: **A. de Castro**, None; **A. Benito**, None; **S. Manzanera**, None; **J. Mompeán**, None; **B. Cañizares**, None; **D. Martínez**, None; **J.M. Marín**, None; **I. Grulkowski**, None; **P. Artal**, None

References

1. Thylefors B. The World Health Organization's programme for the prevention of blindness. *Int Ophthalmol*. 1990;14:211–219.
2. Remington LA. *Clinical Anatomy and Physiology of the Visual System*. 3rd ed. St. Louis, MO: Elsevier, Inc. Butterworth Heinemann; 2011.
3. Cruickshanks KJ, Klein BE, Klein R. Ultraviolet light exposure and lens opacities: the Beaver Dam Eye Study. *Am J Public Health*. 1992;82:1658–1662.
4. Brown NP, Harris ML, Shun-Shin GA, Vrensen GF, Willekens B, Bron AJ. Is cortical spoke cataract due to lens fibre breaks? The relationship between fibre folds, fibre breaks, waterclefts and spoke cataract. *Eye (Lond)*. 1993;7:672–679.
5. Vrensen G, Willekens B. Biomicroscopy and scanning electron microscopy of early opacities in the aging human lens. *Invest Ophthalmol Vis Sci*. 1990;31:1582–1591.
6. Adamsons I, Muñoz B, Enger C, Taylor HR. Prevalence of lens opacities in surgical and general populations. *Arch Ophthalmol*. 1991;109:993–997.
7. Sparrow JM, Bron AJ, Brown NAP, Ayliffe W, Hill AR. The Oxford clinical cataract classification and grading system. *Int Ophthalmol*. 1986;9:207–225.
8. Sasaki K, Shibata T, Obazawa H, et al. Classification system for cataracts. Application by the Japanese Cooperative Cataract Epidemiology Study Group. *Ophthalmic Res*. 1990;22(suppl 1):46–50.
9. Chylack LT, Wolfe JK, Singer DM, et al. The lens opacities classification system III. *Arch Ophthalmol*. 1993;111:831–836.
10. Barraquer RI, Pinilla Cortes L, Allende MJ, et al. Validation of the nuclear cataract grading system BCN 10. *Ophthalmic Res*. 2017;57:247–251.
11. Ullrich K, Pesudovs K. Comprehensive assessment of nuclear and cortical backscatter metrics derived from rotating Scheimpflug images. *J Cataract Refract Surg*. 2012;38:2100–2107.
12. Domínguez-Vicent A, Birkeldh U, Carl-Gustaf L, Nilson M, Brautaset R. Objective assessment of nuclear and cortical cataracts through Scheimpflug images: agreement with the LOCS III scale. *PLoS One*. 2016;11:e0149249.
13. Qian W, Soderberg PG, Chen E, Magnius K, Philipson B. A common lens nuclear area in Scheimpflug photographs. *Eye*. 1993;7:799–804.
14. Grewal DS, Grewal SPS. Clinical applications of Scheimpflug imaging in cataract surgery. *Saudi J Ophthalmol*. 2012;26:25–32.
15. Pei X, Bao Y, Chen Y, Li X. Correlation of lens density measured using the Pentacam Scheimpflug system with the Lens Opacities Classification System III grading score and visual acuity in age-related nuclear cataract. *Br J Ophthalmol*. 2008;92:1471–1475.
16. Duncan DD, Shukla OB, West SK, Schein OD. New objective classification system for nuclear opacification. *J Opt Soc Am A Opt Image Sci Vis*. 1997;14:1197–1204.
17. Kim YN, Park JH, Tchah H. Quantitative analysis of lens nuclear density using optical coherence tomography (OCT) with a liquid optics interface: correlation between OCT images and LOCS III grading. *J Ophthalmol*. 2016;2016:3025413.
18. Wong AL, Leung CK-S, Weinreb RN, et al. Quantitative assessment of lens opacities with anterior segment optical coherence tomography. *Br J Ophthalmol*. 2009;93:61–65.
19. Dicarlo CD, Roach WP, Gagliano DA, et al. Comparison of optical coherence tomography imaging of cataracts with histopathology. *J Biomed Opt*. 1999;4:450–458.
20. Dubbelman M, van der Heijde RGL, Weeber HA, Vrensen GFJM. Changes in the internal structure of the human crystalline lens with age and accommodation. *Vision Res*. 2003;43:2363–2375.
21. Vivino MA, Chintalagiri S, Trus B, Datiles M. Development of a Scheimpflug slit lamp camera system for quantitative densitometric analysis. *Eye (Lond)*. 1993;7:791–798.
22. Xu K, Hao Y. Determination of the density of human nuclear cataract lenses. *Mol Med Rep*. 2013;8:1300–1304.
23. Pierscionek BK, Weale RA. Polarising light biomicroscopy and the relation between visual acuity and cataract. *Eye (Lond)*. 1995;9:304–308.
24. Tsui PH, Huang CC, Zhou Q, Shung KK. Cataract measurement by estimating the ultrasonic statistical parameter using an ultrasound needle transducer: an in vitro study. *Physiol Meas*. 2011;32:513–522.
25. Caixinha M, Jesus DA, Velte E, Santos MJ, Santos JB. Using ultrasound backscattering signals and Nakagami statistical distribution to assess regional cataract hardness. *IEEE Trans Biomed Eng*. 2014;61:2921–2929.
26. Caixinha M, Amaro J, Santos M, Perdigao F, Gomes M, Santos J. In-vivo automatic nuclear cataract detection and classification in an animal model by ultrasounds. *IEEE Trans Biomed Eng*. 2016;63:2326–2335.
27. Al-Khateeb G, Shajari M, Vunnava K, Petermann K, Kohnen T. Impact of lens densitometry on phacoemulsification parameters and usage of ultrasound energy in femtosecond laser-assisted lens surgery. *Can J Ophthalmol*. 2017;52:331–337.
28. Franssen L, Coppens JE, van den Berg TJ. Compensation comparison method for assessment of retinal straylight. *Invest Ophthalmol Vis Sci*. 2006;47:768–776.
29. Artal P, Benito A, Pérez GM, et al. An objective scatter index based on double-pass retinal images of a point source to classify cataracts. *PLoS One*. 2011;6:e16823.
30. Martinez-Roda JA, Vilaseca M, Ondategui JC, et al. Double-pass technique and compensation-comparison method in eyes with cataract. *J Cataract Refract Surg*. 2016;42:1461–1469.

Investigative Ophthalmology & Visual Science